13

Neutron Detectors

T. W. Crane and M. P. Baker

13.1 MECHANISMS FOR NEUTRON DETECTION

Mechanisms for detecting neutrons in matter are based on indirect methods. Neutrons, as their name suggests, are neutral. Also, they do not interact directly with the electrons in matter, as gamma rays do. The process of neutron detection begins when neutrons, interacting with various nuclei, initiate the release of one or more charged particles. The electrical signals produced by the charged particles can then be processed by the detection system.

Two basic types of neutron interactions with matter are available. First, the neutron can be scattered by a nucleus, transferring some of its kinetic energy to the nucleus. If enough energy is transferred, the recoiling nucleus ionizes the material surrounding the point of interaction. This mechanism is only efficient for neutrons interacting with light nuclei. In fact, only hydrogen and helium nuclei are light enough for practical detectors. Second, the neutron can cause a nuclear reaction. The products from these reactions, such as protons, alpha particles, gamma rays, and fission fragments, can initiate the detection process. Some reactions require a minimum neutron energy (threshold), but most take place at thermal energies. Detectors exploiting thermal reactions are usually surrounded by moderating material to take maximum advantage of this feature.

Detectors employing either the recoil or reaction mechanism can use solid, liquid, or gas-filled detection media. Although the choice of reactions is limited, the detecting media can be quite varied, leading to many options. This chapter describes gas-filled proportional counters, scintillators, fission chambers, ^{10}B-lined chambers, and other types of neutron detectors. Gas detectors are discussed in the order of their frequency of use in Sections 13.4.1 through 13.4.4; plastic and liquid scintillators, in Section 13.5; and other types of detectors, in Section 13.6.

The energy information obtained in neutron detection systems is usually poor because of the limitations of the available neutron-induced reactions. Recoil-type counters measure only the first interaction event. The full neutron energy is usually not deposited in the detector, and the only energy information obtained is whether a high- or low-energy neutron initiated the interaction. Reaction-type counters take advantage of the increased reaction probability at low neutron energies by moderating the incoming neutrons. But knowledge of the initial neutron energy before moderation is lost. The energy recorded by the detector is the reaction energy (plus, perhaps, some of the remaining initial neutron energy). Thus, in general, neutron detectors provide information only on the number of neutrons detected and not on their energy. Information on

the range of detected neutron energies can usually be inferred from the detector type and the surrounding materials. If information on the neutron energy spectrum is needed, it can sometimes be obtained indirectly, as discussed in Section 13.7.

13.2 GENERAL PROPERTIES OF GAS-FILLED DETECTORS

Gas-filled detectors were among the first devices used for radiation detection. They may be used to detect either thermal neutrons via nuclear reactions or fast neutrons via recoil interactions. After the initial interaction with the neutron has taken place, the remaining detection equipment is similar, although there may be changes in high-voltage or amplifier gain settings to compensate for changes in the magnitude of the detected signal. Figure 13.1 shows a typical setup for neutron counting with a gas-filled detector. Figure 13.2 shows some commonly used detectors.

The exterior appearance of a gas detector is that of a metal cylinder with an electrical connector at one end (occasionally at both ends for position-sensitive measurements). The choice of connector depends on the intended application; simple wire leads and most other common types are available. Detector walls are about 0.5 mm thick and are manufactured from either stainless steel or aluminum. The performance of either material is quite satisfactory, with only slight differences in neutron transmission or structural strength. Steel walls absorb about 3% of the neutrons; aluminum walls, about 0.5%. Thus, aluminum tubes are usually preferred because of their higher detection

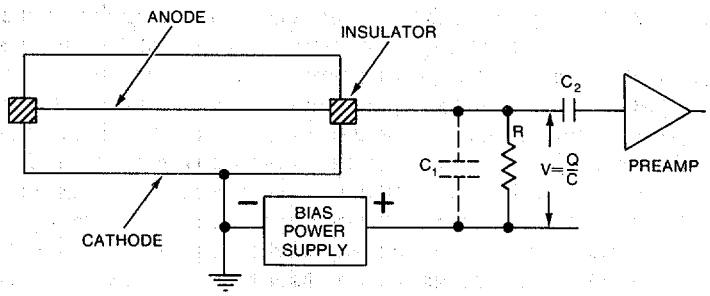

***Fig. 13.1** Typical setup for gas-filled neutron detectors.*

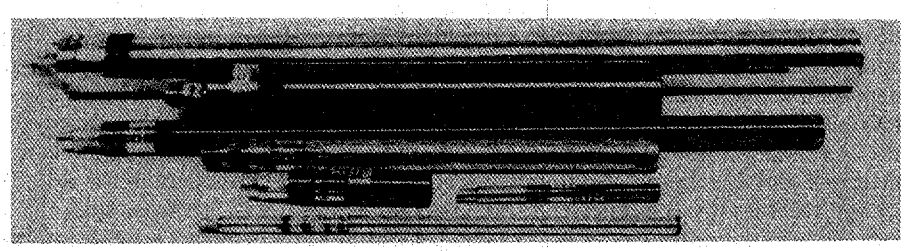

***Fig. 13.2** Various sizes of BF_3 and ^3He neutron detectors.*

efficiency. However, steel tubes have some small advantages over aluminum tubes for certain applications: they require less careful handling during assembly, the connecting threads are less susceptible to galling, and impurities can be kept lower. In very low count-rate applications, a background of about 1 count/min has been observed and attributed to radium impurity in aluminum (Ref. 1).

The central wire shown in Figure 13.1 is typically 0.03-mm-thick gold-plated tungsten. Tungsten provides tensile strength for the thin wire, and the gold plating offers improved electrical conductivity. The wire is held in place by ceramic insulators.

Sometimes the interior walls are coated with activated charcoal. This coating is used for tubes filled with boron trifluoride (BF_3) gas and also for ^{3}He-filled tubes operated in high neutron fluxes. The activated charcoal serves to absorb electronegative gases that build up during neutron irradiation. For example, in a BF_3-filled detector three fluorine atoms are released with each neutron capture. The fluorine atoms will combine with electrons released in subsequent neutron captures. Initially, this process reduces the electric pulse amplitude and eventually output pulses are eliminated altogether (Ref. 2). Additional details on the design of gas-filled detectors are given in Refs. 3 and 4.

As described in Section 13.1, the detection of neutrons requires the transfer of some or all of the neutrons' energy to charged particles. The charged particle will then ionize and excite the atoms along its path until its energy is exhausted. In a gas-filled detector, approximately 30 eV is required to create an ion pair. The maximum number of ion pairs produced is then E/30 eV, where E is the kinetic energy of the charged particle(s) in eV. For example, an energy transfer of 765 keV will release a total positive and negative charge of about 8×10^{-15} coulombs.

If little or no voltage is applied to the tube, most of the ions will recombine and no electrical output signal is produced. If a positive voltage is applied to the central wire (anode), the electrons will move toward it and the positively charged ions will move toward the tube wall (cathode). An electrical output signal will be produced whose magnitude depends on the applied voltage, the geometry of the counter, and the fill gas. These parameters determine whether the detector operates in the ionization region, the proportional region, or the Geiger-Mueller region. These different operating regions are shown in Figure 13.3.

In the ionization region, enough voltage has been applied to collect nearly all the electrons before they can recombine. At this point, a plateau is reached and further small increases in voltage yield no more electrons. Detectors operated in this region are called ion chambers. The charge collected is proportional to the energy deposited in the gas and independent of the applied voltage.

The region beyond the ionization region is called the proportional region. Here the electric field strength is large enough so that the primary electrons can gain sufficient energy to ionize the gas molecules and create secondary ionization. If the field strength is increased further, the secondary electrons can also ionize gas molecules. This process continues rapidly as the field strength increases, thus producing a large multiplication of the number of ions formed during the primary event. This cumulative amplification process is known as avalanche ionization. When a total of "A" ion pairs result from a single primary pair, the process has a gas amplification factor of A. "A" will be unity in an ionization chamber where no secondary ions are formed and as high as 10^3 to 10^5 in a well-designed proportional counter. Note that in the proportional region the charge collected is also linearly proportional to the energy deposited in the gas.

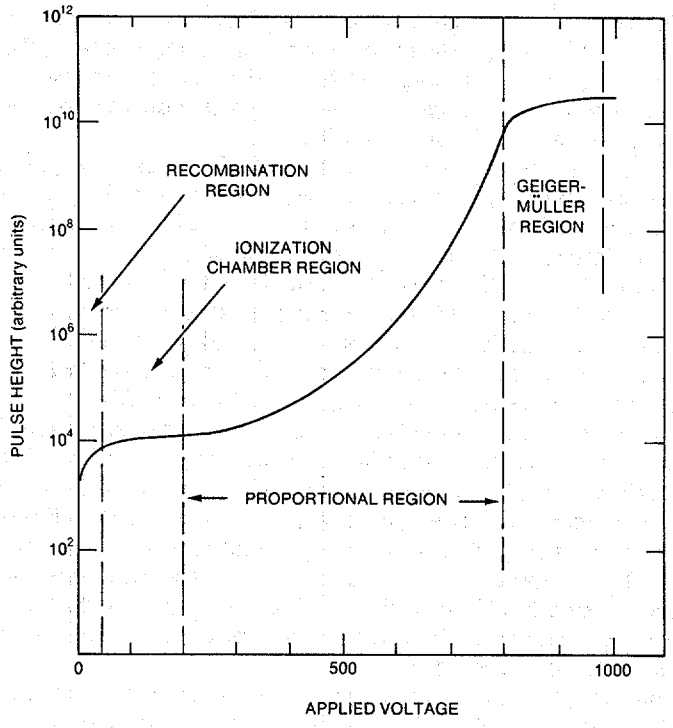

Fig. 13.3 *Pulse-height vs applied-voltage curves to illustrate ionization, proportional, and Geiger-Mueller regions of operation.*

For the amplification process to proceed, an electron must acquire sufficient energy, in one or more mean free paths, to ionize a neutral molecule. The mean free path is the average distance the electron travels between collisions in proportional-counter gas and equals approximately 1 to 2 μm. For amplifications of 10^6, fewer than 20 mean free paths are necessary, which indicates that only a small region around the wire is involved in the multiplication process. In the rest of the volume, the electrons drift toward the anode. Because the amplification process requires a very high electric field, an advantage of the cylindrical detector design is the high electric field near the inner wire. The total amplification will be proportional to the electric field traversed, not the distance traversed.

At the same time that the electrons are drifting toward the anode, the positive ions are drifting toward the cathode. In a proportional counter, the drift velocity of the electrons is approximately 3 orders of magnitude larger than the drift velocity of the positive ions. Because the avalanche is formed near the anode wire, the electrons with a larger drift velocity are collected in an extremely short time interval (within 10^{-8} s); the slower drifting positive ions are collected on the cathode over a much longer time interval. The pulses observed have an initial fast risetime because of the motion of the electrons and a

subsequent slower risetime because of the motion of the positive ions. In addition, because the positive ions are initially formed close to the anode and must drift across the entire anode-to-cathode gap, the pulse amplitude is largely due to the drifting of the positive ions. The pulse reaches full amplitude only when the positive ions are fully collected. For a typical proportional counter this collection process may take 200 μs. Through differentiation, the pulse can be made much shorter without a substantial loss of pulse height so that rapid counting is possible. It is possible to approach the time dispersion caused by the variation in the drift time of the primary electrons from the interaction site to the anode wire. This time dispersion depends on tube voltage and diameter and has been reported (Ref. 5) as 1.1 μs (CH_4), 2.5 μs (^3He), and 17 μs (^4He) for some typical gas-filled tubes.

As the applied voltage is increased further, the proportionality between the primary charge deposited and the output signal is gradually lost. This loss is primarily due to saturation effects at the anode wire. As the primary ions reach the high field regions near the anode wire, the avalanche process begins and quickly grows to a maximum value as secondary electrons create additional avalanches axially along the wire. Unlike operation in the proportional region where the avalanche is localized, the avalanche now extends the full length of the anode wire and the multiplication process terminates only when the electrostatic field is sufficiently distorted to prevent further acceleration of secondary electrons. For weakly ionizing primary events, amplification factors of up to 10^{10} are possible. Detectors operated in this region are called Geiger-Mueller counters. Geiger counters require very simple electronics and form the basis for rugged field inspection instruments. Because they are saturated by each event, Geiger counters cannot be used in high-count-rate applications, but this limitation does not interfere with their use as low-level survey meters.

Neutron counters operated in either the ionization or proportional mode can provide an average output current or individual pulses, depending on the associated electronics. Measuring only the average output current is useful for radiation dosimetry and reactor power monitors. For assay of nuclear material it is customary to operate neutron counters in the pulse mode so that individual neutron events can be registered.

Gas-filled detectors typically employ ^3He, ^4He, BF_3, or CH_4 as the primary constituent, at pressures of less than 1 to about 20 atm depending on the application. Other gases are often added to improve detector performance. For example, a heavy gas such as argon can be used to reduce the range of the reaction products so that more of their kinetic energy is deposited within the gas and, thereby, the output pulse-height resolution is improved. Adding a heavy gas also speeds up the charge collection time, but has the adverse effect of increasing the gamma-ray sensitivity (Ref. 6).

A polyatomic gas may also be added to proportional counters to serve as quench gas. The rotational degrees of freedom available to polyatomic gas molecules serve to limit the energy gained by electrons from the electric potential, thus helping to dampen and shorten the avalanche process and improve the pulse-height resolution. Gases such as BF_3 and CH_4 are already polyatomic gases and require no additional quench gas. Tubes filled with ^3He and ^4He often have a small quantity of CH_4 or CO_2 added. Because BF_3 and CH_4 gases are polyatomic, detectors filled with these gases require higher operating voltages. Also, the relatively large quantity of polyatomic gas restricts the intercollisional energy gain so that these detectors are usually not operated at fill pressures as high as those used for detectors filled with monoatomic gases.

13.3 GAMMA-RAY SENSITIVITY OF NEUTRON DETECTORS

The neutron detectors described in this chapter are sensitive in some degree to gamma rays as well as neutrons. Because most nuclear material emits 10 or more times as many gamma rays as neutrons, the gamma-ray sensitivity of a neutron detector is an important criterion in its selection. For measurements of spent fuel, where gamma-ray fluxes of 1000 R/h or more are encountered, the gamma-ray sensitivity of the detector may dominate all other considerations.

In any detector, gamma rays can transfer energy to electrons by Compton scattering (see Chapter 2), just as neutrons transfer energy to other nuclei by scattering or nuclear reactions. Compton scattering can take place in the detector walls or the fill gas, yielding a high-energy electron that in turn produces a column of ionization as it traverses the detector. In some detectors, electronic pulses induced by gamma rays are comparable in size to neutron-induced pulses; in other detectors, they are much smaller, but can pile up within the resolving time of the electronics to yield pulses comparable to neutron pulses. Four factors should be considered when evaluating the relative magnitudes of the neutron and gamma-ray signals:

(1) The presence of gamma-ray shielding has a substantial effect on the relative magnitude of the signals. For example, for a detector exposed to 1-MeV fission neutrons in the presence of 1-MeV fission gamma rays, 5 cm of lead shielding absorbs roughly 0.1% of the neutrons and 90% of the gamma rays.

(2) Some detector materials and designs favor the absorption of neutrons. Table 13-1 gives examples for thermal- and fast-neutron detectors. From the table it is clear that thermal neutrons can be absorbed with much higher probability than gamma rays. For fast-neutron detection, the neutron and gamma-ray interaction probabilities are comparable.

Table 13-1. Neutron and gamma-ray interaction probabilities in typical gas proportional counters and scintillators

	Interaction Probability	
Thermal Detectors	Thermal Neutron	1-MeV Gamma Ray
^{3}He (2.5 cm diam, 4 atm)	0.77	0.0001
Ar (2.5 cm diam, 2 atm)	0.0	0.0005
BF_3 (5.0 cm diam, 0.66 atm)	0.29	0.0006
Al tube wall (0.8 mm)	0.0	0.014
	Interaction Probability	
Fast Detectors	1-MeV Neutron	1-MeV Gamma Ray
^{4}He (5.0 cm diam, 18 atm)	0.01	0.001
Al tube wall (0.8 mm)	0.0	0.014
Scintillator (5.0 cm thick)	0.78	0.26

Table 13-2. Neutron and gamma-ray energy deposition in typical gas proportional counters and scintillators

Thermal Detectors	Alpha or Proton Range (cm)	dE/dx for 400-keV Electron (keV/cm)	Average Neutron Reaction Energy Deposited (keV)	Electron Energy Deposited (keV)[a]	Ratio of Neutron to Electron Energy Deposition
^{3}He (2.5 cm diam, 4 atm)	2.1	1.1	~500	4.0	125
^{3}He (2.5 cm diam, 4 atm) + Ar (2 atm)	0.5	6.7	~750	24.0	30
BF_3 (5.0 cm diam, 0.66 atm)	0.7	3.6	~2300	25.7	90
Fast Detectors					
^{4}He (5.0 cm diam, 18 atm)	0.1	6.7	1000	48	20
Scintillator (5.0 cm thick)	0.001	2000	1000	400	2.5

[a]This calculation assumes a path length of $\sqrt{2} \times$ tube diameter.

(3) In some detectors neutrons deposit more energy than gamma rays do. Neutrons may induce a nuclear reaction that releases more energy than the Compton scattering of the gamma ray imparts to the electron. (The average energy imparted by a 1-MeV gamma ray is roughly 400 keV). Also, in gas detectors the range of the electron is typically much longer than the range of the heavy charged particles produced by neutron interactions. When the gas pressure is chosen to just stop the heavy charged particles, the electrons will escape from the tube after depositing only a small fraction of their energy in the gas. Table 13-2 gives some numerical examples of these effects. The table also shows that for fast-neutron detection by plastic scintillators the relative neutron and gamma-ray energy deposition is comparable.

(4) The charge collection speeds for neutron and gamma-ray detection may be different. This effect is very dependent on the choice of fill gas or scintillator material. In gas detectors, the long range of the electron produced by a gamma-ray interaction means that energy will be deposited over a greater distance, and more time will be required to collect it. An amplifier with fast differentiation will then collect relatively less of the charge released by a gamma-ray interaction than a neutron interaction. In scintillators, there is less distinction between the two kinds of events. In some circumstances, however, pulse-shape discrimination between neutrons and gamma rays can be achieved (see Section 13.5.3).

To achieve good gamma-ray discrimination, it is often necessary to use materials or material densities that are not optimum for neutron detection. The result may be a reduced neutron detection efficiency. Table 13-3 lists the neutron detection efficiency and approximate gamma-ray radiation limit for various neutron detector types. The detection efficiency is for a single pass through the detector at the specified energy. The actual efficiency for a complete detector system depends on the geometry, and the obtainable efficiency can be lower than the estimate given in Table 13-3. Additional details on these detectors and their gamma-ray sensitivity are given in the following sections.

Table 13-3. Typical values of efficiency and gamma-ray sensitivity for some common neutron detectors

Detector Type	Size	Neutron Active Material	Incident Neutron Energy	Neutron Detection Efficiency[a] (%)	Gamma-Ray Sensitivity (R/h)[b]
Plastic scintillator	5 cm thick	^{1}H	1 MeV	78	0.01
Liquid scintillator	5 cm thick	^{1}H	1 MeV	78	0.1
Loaded scintillator	1 mm thick	^{6}Li	thermal	50	1
Hornyak button	1 mm thick	^{1}H	1 MeV	1	1
Methane (7 atm)	5 cm diam	^{1}H	1 MeV	1	1
^{4}He (18 atm)	5 cm diam	^{4}He	1 MeV	1	1
^{3}He (4 atm), Ar (2 atm)	2.5 cm diam	^{3}He	thermal	77	1
^{3}He (4 atm), CO_2 (5%)	2.5 cm diam	^{3}He	thermal	77	10
BF_3 (0.66 atm)	5 cm diam	^{10}B	thermal	29	10
BF_3 (1.18 atm)	5 cm diam	^{10}B	thermal	46	10
^{10}B-lined chamber	0.2 mg/cm^2	^{10}B	thermal	10	10^3
Fission chamber	2.0 mg/cm^2	^{235}U	thermal	0.5	$10^6 - 10^7$

[a]Interaction probability for neutrons of the specified energy striking the detector face at right angles.
[b]Approximate upper limit of gamma-ray dose that can be present with detector still providing usable neutron output signals.

13.4 GAS-FILLED DETECTORS

13.4.1 ^{3}He and BF_3 Thermal-Neutron Detectors

Gas-filled thermal-neutron detectors use either BF_3 or ^{3}He. In the case of BF_3, the gas is enriched in ^{10}B. Helium-3 is only about 1 ppm of natural helium, so it is usually obtained by separation from tritium produced in reactors. The nuclear reactions that take place in these gases are

$$^{3}He + n \rightarrow {}^{3}H + {}^{1}H + 765\ keV \qquad (13\text{-}1)$$

$$^{10}B + n \rightarrow {}^{7}Li^* + {}^{4}He + 2310\ keV$$

$$\text{and } {}^{7}Li^* \rightarrow {}^{7}Li + 480\ keV \ . \qquad (13\text{-}2)$$

These reactions are exothermic and release energetic charged particles into the gas. The counters are operated in the proportional mode, and the ionization produced by these particles initiates the multiplication process that leads to detection. The amount of energy deposited in the detector is the energy available from the nuclear reaction.

In the case of ^{3}He, the neutron causes the breakup of the nucleus into a tritium nucleus, ^{3}H, and a proton, ^{1}H. The triton and the proton share the 765-keV reaction energy. In the case of ^{10}B, the boron nucleus breaks up into a helium nucleus (alpha

particle) and a lithium nucleus, with 2310 keV shared between them. Ninety-four percent of the time the lithium nucleus is left in an excited state from which it subsequently decays by emitting a 480-keV gamma ray. This gamma ray is usually lost from the detector, in which case only 2310 keV is deposited. About 6% of the time the lithium nucleus is left in the ground state, so that 2790 keV is deposited in the detector. This double reaction mode yields an additional small full-energy peak in the pulse-height spectrum of BF_3 tubes.

The cross section for the ^3He reaction (Equation 13-1) is 5330 b for thermal neutrons, and the cross section for the ^{10}B reaction (Equation 13-2) is 3840 b. Both reaction cross sections are strongly dependent on the incident neutron energy E and have roughly a $1/\sqrt{E}$ dependence. Figure 13.4 illustrates these cross sections (Ref. 7). As an example, a 2.54-cm-diam tube with 4 atm of ^3He has a 77% efficiency for thermal neutrons (0.025 eV). (This configuration is nearly optimum for thermal neutrons; more ^3He would give relatively little additional efficiency and would usually not be cost-effective.) At 100 eV the efficiency is roughly 2%; at 10 keV, roughly 0.2%; and at 1 MeV, roughly 0.002%. Because of this strong energy dependence, it is customary to embed ^3He or BF_3 detectors in approximately 10 cm of polyethylene or other moderating materials to maximize their counting efficiency (see Chapter 14 for additional details on detector design).

Figure 13.5 is a typical pulse-height spectrum from a ^3He proportional counter (Ref. 8). The shape of this spectrum is due primarily to (1) the kinematics of the reaction process and (2) the choice of amplifier time constants. The full-energy peak in the spectrum represents the collection of the kinetic energy of both the proton and the triton. (It should be emphasized that this peak represents the 765 keV released in the reaction and is not a measure of the incident neutron energy.) If one or the other particle enters the tube wall, less energy is collected in the gas, which results in a low-energy tail. Since the two charged particles are emitted back-to-back, one or the other is almost certain to

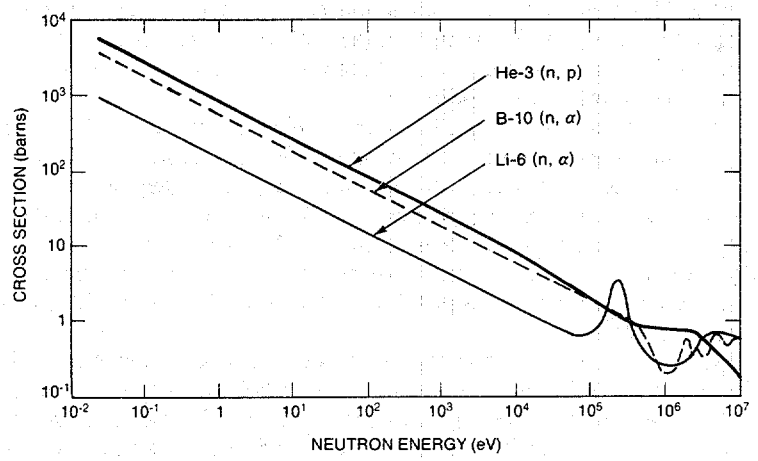

Fig. 13.4 *$^3He(n,p)$, $^{10}B(n,\alpha)$, and $^6Li(n,\alpha)$ cross sections as a function of incident neutron energy (Ref. 7).*

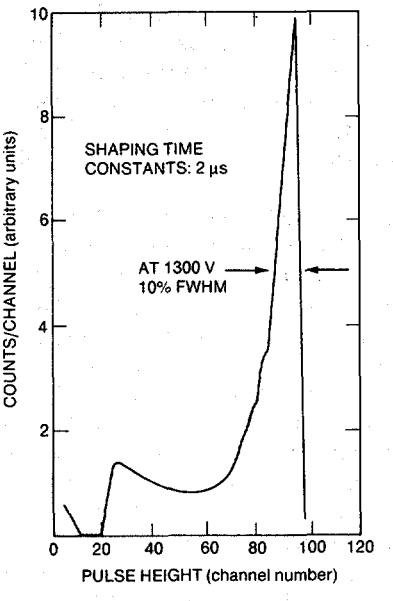

Fig. 13.5 *Differential pulse-height spectrum for thermal neutrons detected by a ^{3}He-filled counter.*

be detected. Thus, there is a minimum collection energy, with a wide valley below, and then a low-energy increase resulting from noise and piled-up gamma-ray events. If the discriminator is set in the valley, small changes in tube voltage or amplifier gain will not affect the count rate. The result is a very stable (approximately 0.1%) detection system.

The choice of amplifier time constant determines the degree of charge collection from the tube. Time constants of 2 μs or greater result in nearly complete charge collection and yield spectra such as the spectrum shown in Figure 13.5, with 5 to 15% resolution (FWHM) of the full-energy peak. Time constants of 0.1 to 0.5 μs cause complete loss of the peak shape, but allow counting at higher rates with less noise pickup and gamma-ray interference. A 0.5-μs time constant is a commonly used compromise between good resolution and high-count-rate capability.

Helium-3 tubes are usually operated in the range of +1200 to 1800 V. Over this range the increase in counting efficiency with voltage caused by improved primary charge collection is very slight, about 1%/100 V (Ref. 8). (A typical plateau curve is shown in Figure 13.6.) On the other hand, the total charge collected (due to multiplication in the gas) changes rapidly with voltage, about 100%/100 V. When ^{3}He tubes are used in multiple detector arrays, it is important to specify good resolution (on the order of 5% FWHM) and uniform gas mixture so that the position and width of the full-energy peak will be the same for all tubes.

A pulse-height spectrum for a BF_3 proportional counter is shown in Figure 13.7 (Ref. 1). For BF_3 tubes, the resolution is in the range 5 to 30% (FWHM) but is usually not as good as for ^{3}He. Gas pressures are in the range 0.2 to 2 atm. To help compensate for the lower pressure, tube diameters are usually 5 cm. Operating voltages are in the range +1400 to 2800 V, higher than for ^{3}He. Plateau curves are similar to those of ^{3}He. BF_3 gas is less expensive than ^{3}He, so that manufacturing costs are less. However, the larger neutron absorption cross section for ^{3}He and the larger possible fill pressure make its

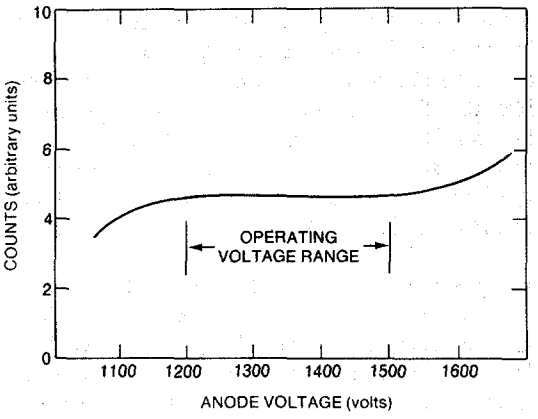

***Fig. 13.6** Typical plateau curve for a gas-filled ^3He counter.*

cost per detected neutron lower in the United States. Another advantage of ^{3}He-filled detectors is that helium is an inert gas whereas BF_3 is toxic. However, US Department of Transportation regulations place detectors with more than 2-atm fill pressure in the high-pressure compressed gas category, so that ^{3}He-filled detectors are often more difficult to ship.

Helium-3 and BF_3 detectors find many applications in passive and active neutron assay because they are relatively stable, efficient, and gamma-insensitive. The detection efficiency for thermal neutrons is high, and the interaction probability for gamma rays is low, as indicated in Table 13-1. Also, much more energy is deposited in the gas by neutron interactions than by gamma-ray interactions, as indicated in Table 13-2. However, if the gamma dose is more than that emitted by typical plutonium and uranium samples, the response of ^{3}He and BF_3 detectors will be affected.

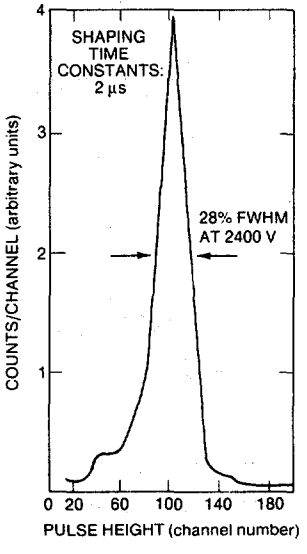

***Fig. 13.7** Differential pulse-height spectrum for thermal neutrons detected by a $^{10}BF_3$-filled counter.*

As an example, Figure 13.8 shows the effect of increasing gamma-radiation fields on a ^{3}He detector (4 atm) containing argon (2 atm) (Ref. 9). The practical operating limit is on the order of 1 R/h. Some improvement can be obtained by replacing argon with about 5% CO_2, as illustrated in Figure 13.9 (Ref. 10). The improvement is due to the removal of the relatively high-Z argon (the electron density is proportional to the Z of the molecule). However, removal of the argon reduces the relative size of the full-energy peak because the reaction products now have longer ranges and deposit less of their energy in the gas. Also, the longer ranges lead to slower charge collection and roughly 35% longer electronic deadtimes.

The gamma-ray sensitivity of BF_3 detectors is comparable to but perhaps slightly better than ^{3}He. The ^{10}B reaction deposits more energy in the gas than the ^{3}He reaction, but gamma-ray interactions also deposit more energy (see Table 13-2). The ^{3}He reaction has a higher cross section than the BF_3 reaction. The cross section for a gamma-ray interaction will depend on the relative amounts of ^{3}He, argon, and BF_3 and on the relative tube wall thicknesses (see Table 13-1). BF_3 detectors can operate in gamma-radiation fields up to 10 R/h, which is better than the performance of ^{3}He + argon counters. However, the performance of ^{3}He + CO_2 counters is comparable to that of BF_3.

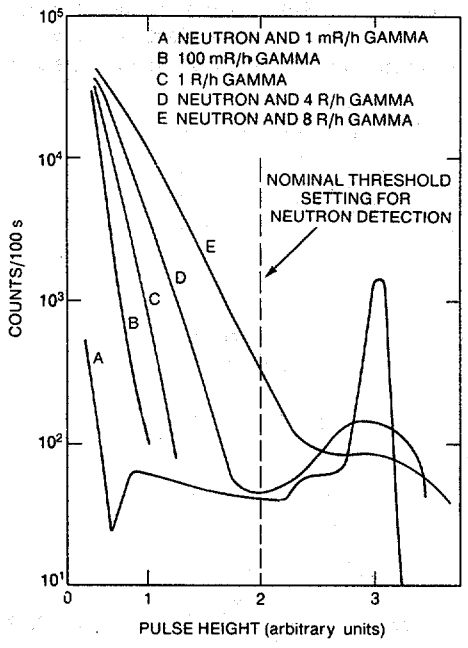

Fig. 13.8 *Gamma-ray pile-up effects for a ^{3}He proportional counter tube 2.54 cm in diameter and 50.8 cm in length.*

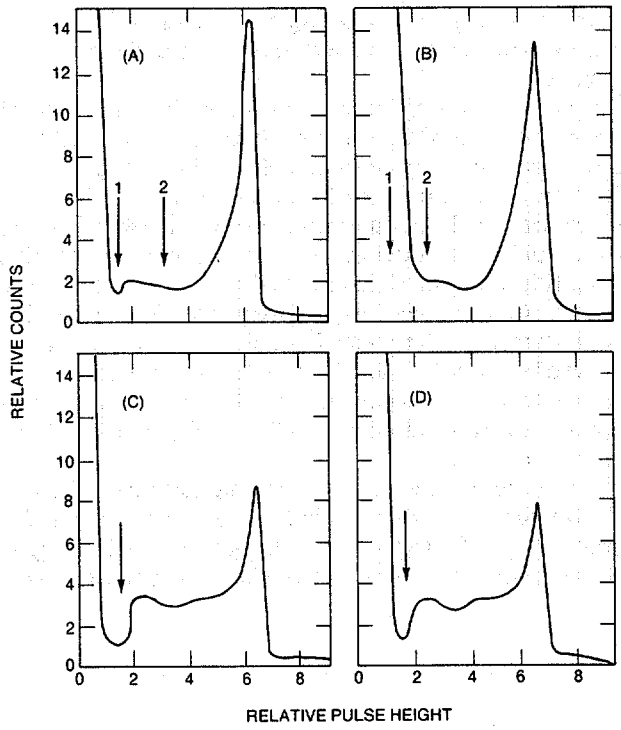

Fig. 13.9 *Differential pulse-height spectra for various ^3He neutron detectors. The amplifier time constant was set at 0.5 μs. (a) $^3He + Ar + CH_4$ mixture with neutron source; (b) $^3He + Ar + CH_4$ mixture with neutron plus 1-R/h gamma-ray source; (c) ^3He + 5% CO_2 mixture with neutron source; (d) ^3He + 5% CO_2 mixture with neutron plus 1-R/h gamma-ray source.*

13.4.2 ^{4}He and CH_4 Fast-Neutron Detectors

Helium-4 and CH_4 fast-neutron detectors rely on the recoil of light nuclei to ionize the gas in the tube. The interaction is the elastic scattering of the neutron by a light nucleus. If the recoiling nucleus is only a hydrogen nucleus (proton), the maximum possible energy transfer is the total neutron kinetic energy E. For heavier elements the maximum energy transfer is always less. For a nucleus of atomic weight A, the maximum energy transfer is (Ref. 7):

$$E(max) = \frac{4A\,E}{(A + 1)^2} \quad . \tag{13-3}$$

For a single scattering event, the actual energy transferred to the recoiling nucleus lies between 0 and E(max) depending on the scattering angle and has equal probability for any value in this range.

Equation 13-3 shows that the target nucleus must have low atomic weight to receive a significant amount of energy from the neutron. Hydrogen is the most obvious choice; it can be used in a gaseous form or, more commonly, in liquid or plastic scintillators (see Section 13.5). Popular gas detectors usually employ methane (CH_4), which has a high hydrogen content, or ^{4}He, which has a maximum energy transfer of 0.64 E(n). (Helium-3 gas is also a suitable candidate by these criteria, but it is usually not used because of the stronger thermal reaction described in Section 13.4.1.) Figure 13.10 illustrates the elastic scattering cross sections for ^{1}H and ^{4}He, showing that they match the shape of the fission-neutron energy spectrum fairly well. Note that the cross sections are substantially lower than those given in Figure 13.4 for ^{3}He and ^{10}B. The efficiency for detecting a fast neutron by an elastic scattering interaction is about 2 orders of magnitude lower than the efficiency for capture of a thermal neutron. Thus a single ^{4}He or CH_4 tube has an intrinsic efficiency of about 1%.

These gas counters are operated as proportional counters with voltages in the range of +1200 to 2400 V. Gas fill pressures are typically 10 to 20 atm for ^{4}He. Relative to ^{4}He, the polyatomic gases CH_4 or H_2 again require higher operating voltages, have slightly lower efficiencies, are limited to lower pressures, and exhibit faster signal risetimes. The

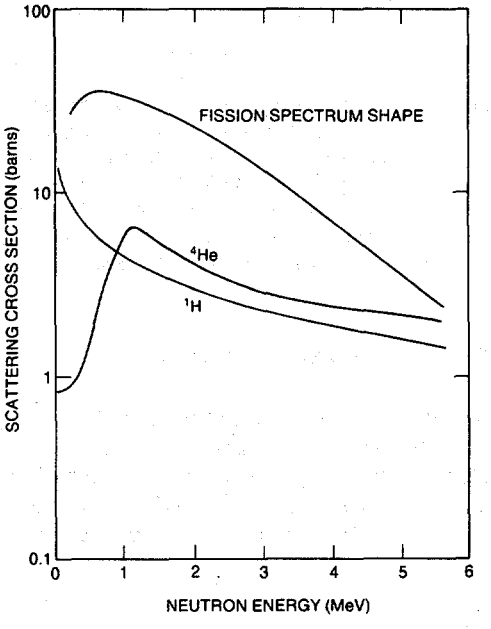

Fig. 13.10 *^{1}H and ^{4}He elastic scattering cross sections, with a fission spectrum shape (not drawn to scale) superimposed.*

gamma-ray sensitivity of the two types of counters is comparable. Neutron counting can be done in gamma-radiation fields of roughly 1 R/h if a moderately high threshold is set (Ref. 11).

Figure 13.11 shows a pulse-height spectrum from a ^{4}He proportional counter collected with a ^{252}Cf neutron source. The observed spectrum shape is the convolution of the following effects:

(1) the ^{252}Cf spontaneous fission neutron spectrum, as illustrated in Figure 11.2,

(2) the probability of transferring an energy between 0 and E(max) to the recoiling nucleus,

(3) the probability of multiple neutron scatterings and the probability of losing recoiling nuclei in the tube walls (see Ref. 12, Figure 8-14 for an example),

(4) the detection of low-energy noise pulses and gamma-ray pile-up events.

Because of these effects the pronounced peak in the initial neutron energy spectrum may be lost, or nearly lost, as indicated in Figure 13.11. Nevertheless, some energy information remains, and more can be obtained by attempting to unfold the above effects. It is customary to set a threshold high enough to reject low-energy noise and gamma-ray events, but low enough to collect many of the medium- and high-energy neutron events. Since the threshold must be set on a sharply falling curve, a recoil detector is not as stable as a thermal detector.

Despite the apparent disadvantages of recoil-type detectors in terms of lower efficiency and stability, the detection process takes place without prior thermalization of the incident neutron. Thus the neutron is detected very rapidly and some information on its initial energy is preserved. Fast-neutron counters can detect neutrons in the energy range of 20 keV to 20 MeV, and some are useful for fast coincidence counting with 10- to 100-ns resolving times. It is also possible to set a threshold that will reject gamma rays and low-energy neutrons, a feature that is particularly suitable for active assay systems.

13.4.3 Fission Chambers

Fission chambers are a variation of the gas-filled counters previously described. They detect neutrons that induce fissions in fissionable material coated on the inner walls of the chamber. Often the exterior appearance of fission chambers is quite similar to that of other gas counters, although they are also available in smaller diameters or in other shapes. The fissionable material is usually uranium highly enriched in ^{235}U. A very thin layer (0.02 to 2 mg/cm^2 surface thickness) is electroplated (sometimes evaporated or painted) on the inner walls. The thin layer is directly exposed to the detector gas. After a

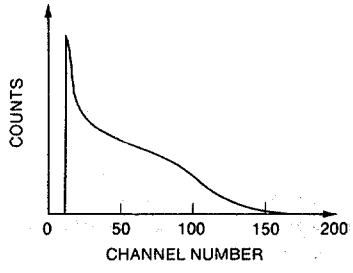

Fig. 13.11 *Differential pulse-height spectrum of ^{4}He proportional counter for a ^{252}Cf source.*

fission event, the two fission fragments travel in nearly opposite directions. The ionization caused by the fission fragment that entered the gas is sensed by the detector; the fragment traveling in the opposite direction is absorbed in the detector walls (Ref. 13).

The two fragments share about 160 MeV of energy, but their range is quite short. For a typical plating material such as uranium, the average fission fragment range is only about 7 μm, equivalent to about 13 mg/cm^2 of coating thickness. Consequently, fission fragments that are produced at a depth of more than 7 μm in the detector wall cannot reach the gas to cause ionization. Furthermore, most fragments exit at a grazing angle, so that their path length is longer than the minimum needed to escape. Because the coating must be kept thin to allow the fission fragments to enter the gas, the fission chamber uses only a small quantity of fissionable material and has a low detection efficiency. For thermal neutrons, the intrinsic efficiency is typically 0.5 to 1%. Fast neutrons can also be detected, but with even lower efficiency.

Fission chambers are operated in the ion chamber mode because the ionization caused by the fission fragments is sufficient and no further charge multiplication within the detector is necessary. The electronics configuration shown in Figure 13.1 is frequently used, with an applied voltage in the +200 to 600 V range. A mixture of 90% argon and 10% methane is a common fill gas. At this pressure the range of fission fragments is about 2 cm.

Figure 13.12 shows a pulse-height spectrum from a ^{235}U chamber (Ref. 14). If energy losses in the coating or in the walls are not too great, the double hump shape caused by light and heavy fission fragments (near 70 and 100 MeV) is visible. Also, an alpha-particle background is present at low energies because nearly all fissionable material contains alpha-emitting isotopes. The alpha-particle energy is typically 5 MeV, whereas the fission fragment energy is an order of magnitude larger. Thus the threshold setting of the counting electronics can be set above the alpha-induced signal. At this threshold setting, some of the low-energy fission-fragment pulses will be lost. Plutonium has a much higher alpha activity than uranium; as a consequence more alpha pulses pile up and the threshold for plutonium-lined fission chambers must be set higher than for uranium-lined chambers.

Because of the large quantity of energy deposited by the fission fragments, fission chambers have the highest insensitivity to gamma rays (roughly 10^6 R/h) of any of the

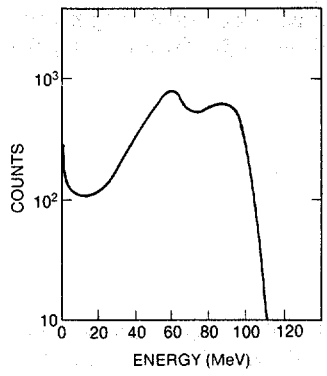

Fig. 13.12 Differential pulse-height spectrum of a ^{235}U fission chamber with a coating thickness of about 0.8 mg/cm^2.

neutron detectors. They are the only detectors capable of direct unshielded neutron measurement of spent reactor fuel. This passive measurement feature applies to both high neutron and gamma-ray fluxes. The inherently low efficiency of fission chambers is compensated for by the large number of neutrons available for counting.

13.4.4 ^{10}B-Lined Detectors

Detectors lined with ^{10}B lie between ^{3}He and $^{10}BF_3$ proportional counters and fission chambers in terms of neutron detection efficiency and gamma-ray insensitivity. Structurally, ^{10}B-lined detectors are similar to fission chambers with the neutron-sensitive material, boron, plated in a very thin layer (about 0.2 mg/cm^2) on the walls of the detector.

The ^{10}B-lined detectors rely on the nuclear reaction given in Equation 13-2 to detect neutrons. Either the alpha particle or the lithium nucleus enters the detection gas (not both, since they are emitted back to back), and the detection process is initiated. Because the range of the alpha particle is about 1 mg/cm^2 in boron, the plating must be thin and the detection efficiency (on the order of 10%) is lower than for BF_3 gas-filled counters. However, since the nuclear reaction does not take place in the fill gas, the gas can be optimized for fast timing. Argon at 0.25 atm pressure, with a small admixture of CO_2, is one common choice. The counter is operated in the proportional mode at a voltage of +600 to 850 V (Ref. 15).

Figure 13.13 shows the pulse-height spectrum of the ^{10}B-lined chamber described above. The stepped structure of the spectrum is caused by the fact that either the alpha particle or the lithium nucleus can enter the gas. Because the lighter alpha particle carries more of the energy, the step resulting from the alpha particle is shown farther to the right. The large number of low-energy pulses is due to the energy loss of the particles in the boron coating of the walls. The detector threshold is usually set above these low-energy

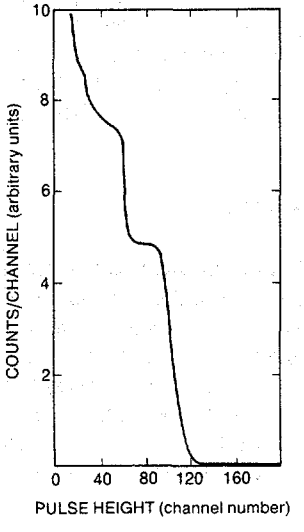

Fig. 13.13 *Differential pulse-height spectrum of a ^{10}B-lined proportional counter.*

pulses. Because there is no well-defined "valley" to set the threshold in, the count-rate plateau curve is roughly 10%/100 V (Ref. 15).

The ^{10}B-lined counter can detect thermal neutrons with moderate efficiency and fast neutrons with low efficiency. It is most useful for applications where it is necessary to detect neutrons in the presence of high gamma-ray fields. With proper electronics, the detector can be operated in a gamma-ray flux as high as 1000 R/h with a 50% loss in neutron detection efficiency resulting from the higher discriminator setting required to reject piled-up gamma events (Ref. 15). The higher gamma-ray insensitivity of the ^{10}B-lined counter relative to the BF_3 gas-filled counter is due to the lower fill pressure and lower operating voltage, which reduce the size of gamma-ray pulses relative to neutron pulses.

13.5 PLASTIC AND LIQUID SCINTILLATORS

13.5.1 Background

Plastic and liquid (organic) scintillators are often used for fast-neutron detection because of their fast response and modest cost. Fast response is particularly beneficial for coincidence counting applications where the ratio of real to accidental coincidence events can have a significant impact on the statistical precision of measurement. Although organic scintillators have response times of a few nanoseconds, the coincidence resolving time for assay applications is usually dictated by the dynamic range of neutron flight times (tens of nanoseconds) from the sample to the detectors. (A 500-keV neutron will traverse a flight path of 1 m in ~100 ns.) The resolving times of coincidence counting systems that moderate fast neutrons prior to detection, on the other hand, are dominated by the dynamic range of times (tens of microseconds) required for thermalization.

The major disadvantage of organic scintillators in nondestructive assay applications is their high gamma-ray sensitivity. Detection probabilities for neutrons and gamma rays are comparable, and the pulse-height spectra resulting from monoenergetic radiation of both types are broad and overlapping. Hence, pulse height alone yields little information about particle type. In certain organic scintillators, however, electronic pulse-shape discrimination techniques can be used to effectively distinguish between neutron and gamma-ray interactions.

13.5.2 Neutron and Gamma-Ray Interaction Mechanisms

Fast neutrons interact in scintillators through elastic scattering with the nuclei present (mostly carbon and hydrogen). For fission spectrum or (α,n) neutrons, most of the useful scintillator light comes from recoiling hydrogen nuclei (protons). This occurs because a neutron can transfer 100% of its energy in an elastic scattering interaction to a recoiling proton but only 28% can be transferred to a recoiling ^{12}C nucleus. The kinetic energy of the recoiling protons is absorbed by the scintillator and is ultimately converted to heat and visible light. The visible light can be collected in a photomultiplier tube optically coupled to the scintillator and converted to an electronic pulse whose magnitude is related to the kinetic energy of the recoiling proton.

A good scintillation material for neutron detection has relatively high efficiency for converting recoil particle energy to fluorescent radiation, good transparency to its own radiation, and good matching of the fluorescent light spectrum to the photomultiplier-tube response. Many commercially available scintillators such as NE102 and NE213 adequately satisfy these criteria. Table 13-4 gives examples of plastic and liquid scintillators that are widely available. The wavelength of maximum scintillation light emission is typically ~400 nm. At that wavelength, light attenuation lengths are in the range 1 to 5 m. Since light can travel relatively long distances in the scintillator material without significant attenuation, organic scintillators with dimensions of the order of 1 m are not uncommon.

Although the mechanism by which fast neutrons transfer their kinetic energy to protons in an organic scintillator is identical to that in a hydrogen or methane recoil proportional counter, a number of features of the overall detection process are markedly different. This distinction is largely due to the differences in physical properties of organic scintillators and gases. The density, for example, of gas in a recoil proportional counter is of order 10^{-3} g/cm^3, whereas that of an organic scintillator is of order unity. This difference in density means that for a given detection path length in the two materials the probability of interaction for both neutrons and gamma rays will be substantially higher in the scintillator than in the proportional counter. Figure 13.14 illustrates the energy dependence of the interaction probability (expressed as attenuation coefficients) for neutron and gamma-ray interactions in NE213. This figure shows, for example, that a 1-MeV neutron has an interaction probability of ~78% in a 5-cm-thick NE213 liquid scintillator, whereas a 1-MeV gamma ray has an interaction probability of ~26%.

In addition, the ranges of the recoiling protons and electrons will be substantially shorter in the scintillator than in the proportional counter. Except for events occurring near the boundaries of the detectors, this fact is of little importance when considering the recoiling protons. However, the shortened range of the recoil electrons in the organic

Table 13-4. Some representative plastic and liquid scintillators for neutron detection

Type	I.D.	Mfg[a]	Light Output (% of anthracene)	Decay Const (ns)	Wavelength of Max. Emission (nm)	H/C Atomic Ratio	Comments
Plastic	NE102A	1	65	2.4	423	1.104	general use
	NE104	1	68	1.9	406	1.100	fast timing
	NE111A	1	55	1.6	370	1.103	ultrafast timing
	Pilot B	1	68	1.8	408	1.100	general use
	Pilot U	1	67	1.4	391	1.100	ultrafast timing
Liquid	NE211	1	78	2.6	425	1.248	general use
	NE213	1	78	3.7	425	1.213	fast n (P.S.D)
	BC501	2	78	3.7	425	1.213	fast n (P.S.D)
	NE228	1	45		385	2.11	high H/C ratio
	NE311	1	65	3.8	425	1.701	boron-loaded
	NE323	1	60	3.8	425	1.377	gadolinium-loaded

[a]Manufacturer code: (1) Nuclear Enterprises, Ltd.; (2) Bicron Corp.

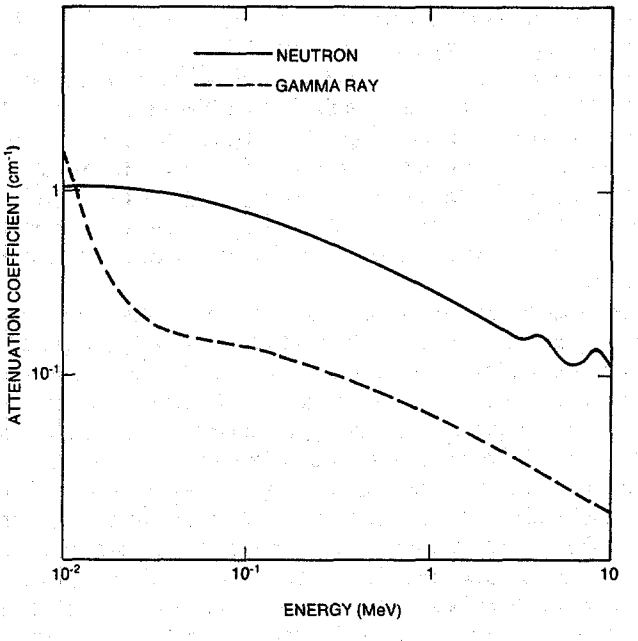

Fig. 13.14 *Attenuation coefficients as a function of incident energy for neutron and gamma-ray interactions in NE213.*

scintillators has a profound effect in that high-energy electrons can stop inside the detection volume. For example, a 500-keV electron can deposit all of its energy in a scintillator while depositing only a small fraction in a gas proportional counter.

Furthermore, recoiling electrons and protons of the same initial energy produce differing amounts of light in a scintillator. This result is apparently due to the differing ionization densities along the slowing-down paths in the two cases. The light output for protons is always less than that for electrons of the same energy, as shown in Figure 13.15 (Refs. 7 and 16). Also, the light output for the two particle types has a different dependence as a function of energy. (Carbon-12 recoils give even less light than proton recoils of the same energy, further reducing their already small contribution to the detection process.) As a rule of thumb, 60-keV electrons and 500-keV protons give approximately equal amounts of light in a typical organic scintillator.

13.5.3 Pulse-Shape Discrimination

The mechanism by which a fraction of the kinetic energy of the recoiling particles is transformed into visible light in an organic scintillator is very complex. However, a few features can be simply stated. The major components of the scintillator light decay in times of the order of a few nanoseconds. This means that, in principle, organic scintillators can operate at very high counting rates. However, there is a weaker, longer-

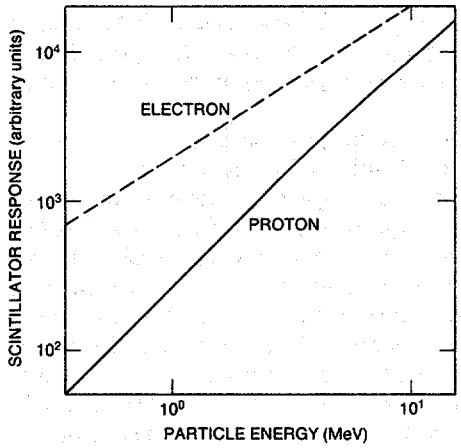

Fig. 13.15 *Scintillation light yield as a function of particle energy for electrons and protons in NE102. The data are taken from Refs. 7 and 16.*

lived component of the radiation from many scintillators that corresponds to delayed fluorescence. Consequently, the total light output can often be represented by the sum of the two exponential decays referred to as the fast and slow components of the scintillation. The slow component has a characteristic decay time in the range of a few hundred nanoseconds. The fraction of the total light observed in this weaker, slower component is a function of the type of particle inducing the radiation. Heavier particles have higher specific ionization and produce more delayed fluorescence light. Figure 13.16 (Ref. 17) illustrates the time dependence of scintillator pulses in stilbene, a solid organic crystal scintillator, when the crystal is excited by different types of radiation.

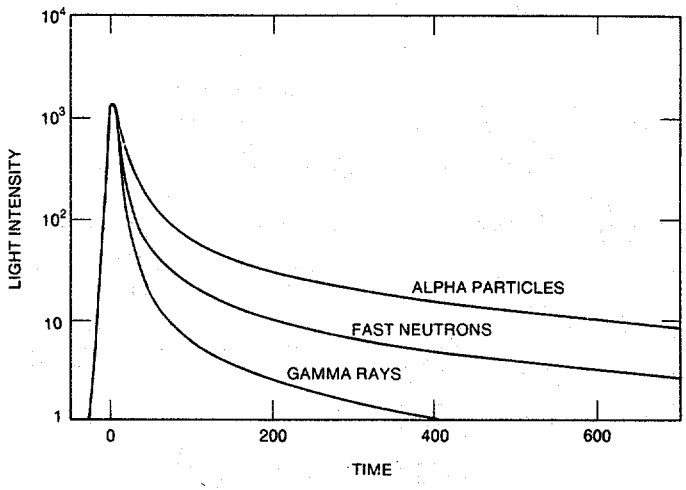

Fig. 13.16 *The time dependence (in nanoseconds) of scintillation pulses in stilbene when excited by different incident particle types (Ref. 17). Note that the light intensity is plotted on a logarithmic scale.*

This time dependence makes it possible to identify particles that have differing rates of energy loss but produce the same amount of light in the scintillator. This procedure is termed pulse-shape discrimination and is used to reject gamma-ray events in neutron detection applications of organic scintillators.

Pulse-shape discrimination is achieved by electronically exploiting the light-emission time-dependence properties of different types of radiation incident on organic scintillators. The most common method used for pulse-shape discrimination in organic scintillators is based on passing the photomultiplier-tube pulse through a bipolar-shaping network, usually a double-delay line. The zero-amplitude crossing of this bipolar pulse depends on the risetime and shape of the initial pulse but is independent of amplitude. Thus, a measure of the pulse shape is given by the time interval between the leading edge of the initial pulse (which is independent of pulse shape) and the zero crossing of the bipolar-shaped pulse. An example of a circuit employing this method is given in Figure 13.17 taken from Ref. 18. Also indicated in the figure are schematic representations of recoil electron and proton pulses at different points in the circuit.

The performance of a pulse-shape discrimination circuit is usually stated in terms of a figure of merit. This measure compares the separation of neutron and gamma-ray-induced events in the time-difference spectrum to the sum of the widths of the individual event distributions as shown in Figure 13.18. The figure of merit is generally reduced by increases in either the dynamic range of processed input pulse heights or the

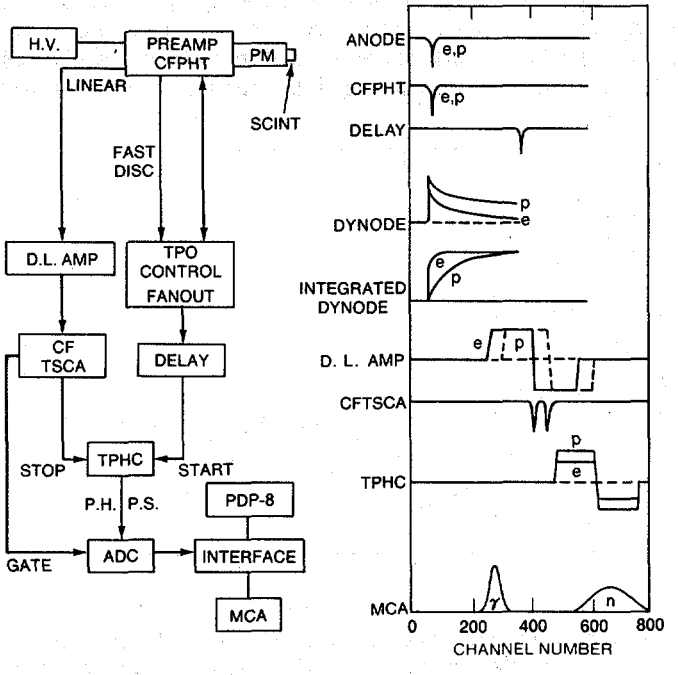

***Fig. 13.17** Pulse-shape discrimination circuit employing the "crossover/leading-edge" time-difference method (Ref. 18).*

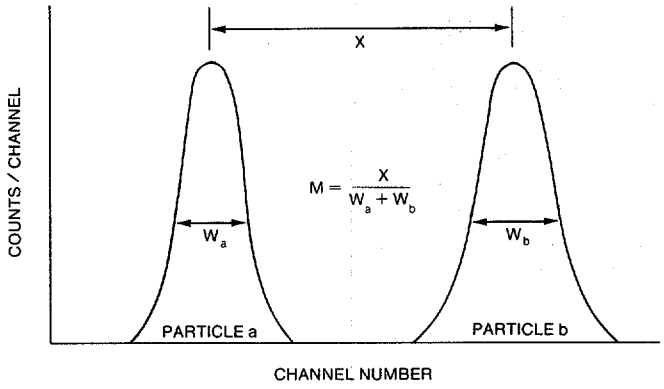

Fig. 13.18 *Illustration of the figure of merit, M, for measuring performance of pulse-shape discrimination systems.*

gross counting rate. Successful operation of pulse-shape discrimination circuits with dynamic ranges of 100 at counting rates of 10^4 s^{-1} have been reported (Ref. 18). Figure 13.19 shows experimental results obtained with an NE218 liquid scintillator and a plutonium-beryllium neutron/gamma-ray source.

Another common approach to pulse-shape discrimination involves integrating the charge contained in the early risetime part of the pulse and comparing it to the integral of the charge in the late part of the pulse. In a recent application (Ref. 19) of this method, the anode pulse from the photomultiplier tube is split and the early and late parts of the pulse are separately gated into integrating analog-to-digital converters. The ratio of the digital results for the late and early parts of the pulse then gives a pulse-shape discrimination spectrum similar to that shown in Figure 13.20.

13.6 OTHER TYPES OF NEUTRON DETECTORS

This section describes several neutron detectors that have not found widespread use for nuclear material assays. Like the other detectors described in this chapter, they rely ultimately on either recoil interactions or direct nuclear reactions to detect neutrons.

Some scintillators are manufactured with neutron-active material added to achieve enhanced neutron detection capability. The purpose is to achieve more localized and more rapid detection of neutrons than is possible with gas counters. Gadolinium, ^{10}B, and ^6Li are typical materials "loaded" into the scintillator. The neutron-active material initiates the light production by releasing energetic charged particles or gamma rays when the neutron is captured. After the initial interaction with the neutron occurs, the detection process is the same as if the light were produced by a gamma ray. Because the scintillator is also a gamma-ray detector, its gamma-ray sensitivity is generally very high. There are, however, several possible configurations with good neutron detection efficiency and low gamma-ray sensitivity.

One useful configuration for thermal-neutron counting consists of lithium-loaded glass scintillators. ZnS(Ag) crystals in a glass medium or cerium-activated silicate glasses

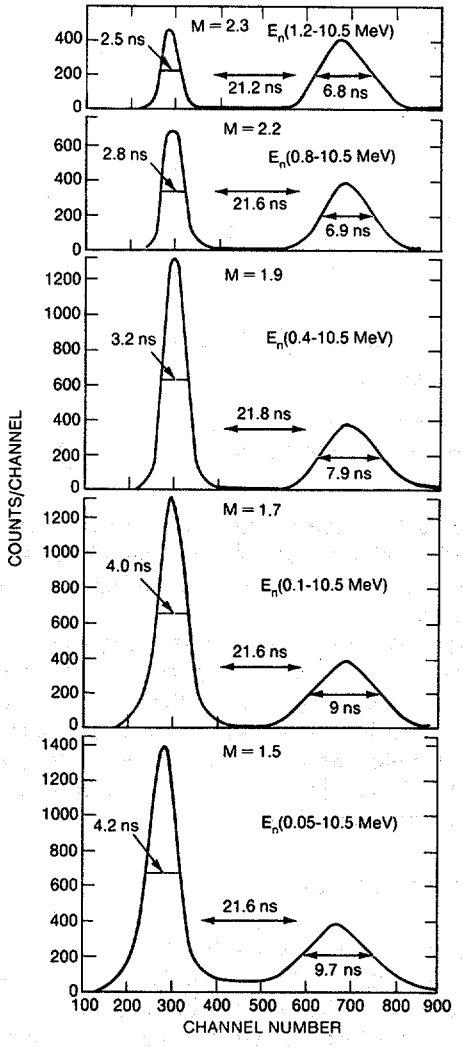

Fig. 13.19 *Risetime distributions for different neutron energy dynamic ranges for an NE218 liquid scintillator and a plutonium-beryllium neutron/gamma-ray source (from Ref. 18).*

are available. Thermal neutrons interact with ^{6}Li via the (n,α) reaction, and the heavy alpha particles excite the scintillator. Detectors of this type are available in sheets with thicknesses of about 1 mm. For thermal neutrons, efficiencies of 25 to 99% are possible in gamma-ray fields on the order of 1 R/h. The low gamma-ray sensitivity is due to the high thermal-neutron capture cross section, the large 4.78-MeV energy release in the reaction, and the thinness of the detector (Ref. 7).

If ZnS(Ag) crystals are dispersed in Lucite, detection of fast neutrons is possible. The interaction mechanism is the elastic scattering of neutrons by hydrogen. The recoiling

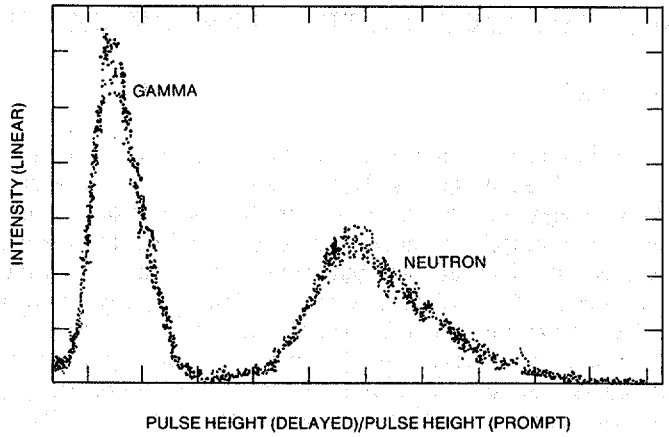

Fig. 13.20 *Ratio of delayed gate ADC conversion to prompt gate ADC conversion for NE213 (Ref. 19).*

proton deposits its energy in the scintillator, and by transfer reactions the ZnS(Ag) crystals are excited. ZnS(Ag) offers good gamma-ray insensitivity because relatively high energies are required to excite the light-emitting property of the zinc sulfide crystals. Detectors that consist of ZnS(Ag) crystals dispersed in Lucite are called Hornyak buttons (Ref. 20); their efficiency is low (on the order of 1%) because the poor light transmission properties of this material limits its use to small sizes. Thin sheets have also been used for measurements of waste crates at the Rocky Flats Plant (Ref. 21). Hornyak buttons can operate in gamma fields up to about 1 R/h because of the properties of ZnS(Ag) and because the thinness of the detector limits the gamma-ray-induced energy deposition.

Most neutron detectors combine neutron-sensitive material and detection electronics into one inseparable unit. However, it is possible to employ a detection system that is more compact and portable by using only the neutron-sensitive material. This material is first placed at the point of interest, then removed for measuring the actual neutron flux by observing isotopic or crystalline structure changes. An example is the use of thermoluminescent dosimeters (TLDs), which consist of crystals that, when heated, emit an amount of light proportional to the dose received. Thermoluminescent dosimeters are primarily used for gamma-ray measurements, but one common crystal, LiF, can be made to be neutron sensitive by increasing the enrichment of ^{6}Li (Ref. 7).

Activation foils, used for criticality safety and low-level detection, provide other examples of the use of neutron-sensitive material. One application has been the use of thin copper sheets to monitor plutonium migration in soil near nuclear waste storage sites (Ref. 22). The technique relies on neutron capture in ^{63}Cu to yield ^{64}Cu, which decays to ^{64}Ni + e^{+} with a 12.7-hour half-life. The foils are buried long enough to achieve an equilibrium level of ^{64}Cu and then retrieved to permit measurement of the positron emission rate. Plutonium concentrations as low as 10 nCi/g have been monitored.

13.7 MEASUREMENT OF NEUTRON ENERGY SPECTRA

13.7.1 Background

As noted in Section 13.1, passive neutron assays are usually based on counting neutrons without regard to their energy. This is because (1) radioactive materials emit neutrons with broad energy spectra that are very similar from one isotope to another and (2) neutron detection is an indirect process that preserves little information about the incident neutron energy. This chapter has shown that neutron detection usually produces a broad spectrum of events that are only indirectly related to the neutron energy. A partial exception is found in the case of recoil detectors such as ^{4}He gas-filled counters and plastic scintillators. However, none of the detectors described in this chapter can distinguish nuclear isotopes on the basis of their neutron energy.

As a consequence, passive neutron assay is usually based on the counting of thermal or fast neutrons, with perhaps some tailoring of the detector or its surroundings to favor a particular broad energy interval. Detectors are also chosen on the basis of their ability to produce fast (10 to 100 ns) or slow (10 to 100 μs) output signals for coincidence counting. Some detectors are also designed to have a detection efficiency that is nearly independent of neutron energy.

13.7.2 Techniques

Although measurement of neutron energy spectra is not necessary for passive neutron assay, it is sometimes important for research or instrument development activities. Such a measurement is difficult, but possible by a variety of techniques. These techniques include proton recoil spectrometers, neutron time-of-flight measurements, and ^{3}He spectrometers. An example of the use of ^{3}He spectrometers in measuring neutron energy spectra follows.

The ^{3}He spectrometer developed by Shalev and Cuttler (Refs. 23 and 24) has been used to measure delayed neutron energy spectra. (The AmLi neutron spectrum given in Figure 11.5 was also measured with an instrument of this type.) The spectrometer is a gas-filled proportional counter containing ^{3}He, argon, and some methane. Neutrons are detected via the ^{3}He (n,p) reaction in the energy range of 20 keV to 2 MeV. In this energy range the reaction cross section is smooth and nearly flat, declining from roughly 10 to 1 b. To detect these fast neutrons the tube is not enclosed in moderating material; rather, it is wrapped in cadmium and boron sheets to reduce the contribution of the much stronger thermal ^{3}He (n,p) reaction (5330 b). Also, a lead shield is often added to reduce the effects of gamma-ray pile-up on the neutron energy resolution. The intrinsic efficiency is low, on the order of 0.1%.

The energy spectrum of a ^{3}He spectrometer includes a full energy peak at the neutron energy E_n + 765 keV, a thermal neutron capture peak at 765 keV, and a ^{3}He (n,n′) elastic scattering recoil spectrum with a maximum at 0.75 E_n (from Equation 13-3). To emphasize the full energy peak at E_n + 765 keV, long charge collection time constants of 5 to 8 μs are used. This favors the slower proton signals from the (n,p) reaction over

the faster signals from recoiling ^{3}He nuclei. It is also helpful to collect data in a two-dimensional array of charge collected vs signal risetime in order to obtain more pulse-shape discrimination. In this way a neutron energy spectrum can be obtained, although it must be carefully unfolded from the measured data.

REFERENCES

1. Engineering Data Sheets 1.21 and 1.22 for BF_3 Proportional Counters (Reuter-Stokes, Inc., Cleveland, Ohio, 1979).

2. A. E. Evans, H. O. Menlove, R. B. Walton, and D. B. Smith, "Radiation Damage to ^{3}He Proportional Counter Tubes," *Nuclear Instruments and Methods* 133, (1976).

3. D. H. Wilkinson, *Ionization Chambers and Counters* (Cambridge University Press, Cambridge, Massachusetts, 1950).

4. P. Rice-Evans, *Spark, Streamer, Proportional, and Drift Chambers* (The Richelieu Press, London, 1974).

5. T. L. Atwell and H. O. Menlove, *Measurement of the Time Resolution of Several ^{4}He and CH_4 Proportional Counters* in "Nuclear Safeguards Research Program Status Report, September—December 1973," Los Alamos Scientific Laboratory report LA-5557-PR (February 1974).

6. T. D. Reilly, "The Measurement of Leached Hulls," Los Alamos Scientific Laboratory report LA-7784-MS (July 1979), pp. 57-63.

7. G. F. Knoll, *Radiation Detection and Measurement* (John Wiley & Sons, Inc., New York, 1979).

8. Engineering Data Sheets 1.02 and 1.03 for ^{3}He Proportional Counters (Reuter-Stokes, Inc., Cleveland, Ohio, 1978).

9. T. W. Crane, "Shielding for ^{3}He Detectors" in "Nuclear Safeguards Research Program Status Report, May—August 1976," Los Alamos Scientific Laboratory report LA-6675-PR (January 1977), p. 3.

10. T. W. Crane, "Gas Mixture Evaluation for ^{3}He Neutron Detectors," in "Nuclear Safeguards Research and Development Program Status Report, May—August 1977," Los Alamos Scientific Laboratory report LA-7030-PR (March 1978), p. 39.

11. M. L. Evans, "NDA Technology for Uranium Resource Evaluation, January 1—June 30, 1978," Los Alamos Scientific Laboratory report LA-7617-PR (1979), pp. 36-41.

12. T. Gozani, *Active Nondestructive Assay of Nuclear Materials, Principles and Applications,* NUREG/CR-0602, SA1-MLM-2585 (US Nuclear Regulatory Commission, Washington, DC, 1981).

13. R. W. Lamphere, "Fission Detectors," in *Fast Neutron Physics,* I, J. B. Marion and J. L. Fowler, Eds. (Interscience Publishers, Inc., New York, 1960).

14. S. Kahn, R. Harman, and V. Forgue, *Nuclear Science and Engineering* 23, 8 (1965).

15. Engineering Data Sheet 1.41 for a ^{10}B-Lined Proportional Counter (Reuter-Stokes Inc., Cleveland, Ohio, 1979).

16. R. L. Craun and D. L. Smith, "Analysis of Response Data for Several Organic Scintillators," *Nuclear Instruments and Methods* 80, 239 (1970).

17. L. M. Bollinger and G. E. Thomas, *Review of Scientific Instruments* 32, 1044 (1961).

18. D. W. Glasgow, D. E. Velkley, J. D. Brandenberger, and M. T. McEllistrem, "Pulse-Shape Discrimination for Wide Dynamic Range Neutron Scattering Experiments," *Nuclear Instruments and Methods* 114, 535 (1974).

19. C. L. Morris, J. E. Bolger, G. W. Hoffman, C. F. Moore, L. E. Smith, and H. A. Thiessen, "A Digital Technique for Neutron-Gamma Pulse Shape Discrimination," *Nuclear Instruments and Methods* 137, 397 (1976).

20. W. F. Hornyak, "A Fast Neutron Detector," *Review of Scientific Instruments* 23 (6), 264 (1952).

21. R. A. Harlan, "Uranium and Plutonium Assay of Crated Waste by Gamma-Ray, Single Neutron, and Slow Coincidence Counting," in Proc. American Nuclear Society Topical Conference on Measurement Technology for Safeguards and Materials Control, Kiawah Island, South Carolina, November 26-28, 1979 (National Bureau of Standards Publication 582, 1980), p. 622.

22. L. E. Bruns, "Capability of Field Instrumentation to Measure Radionuclide Limits," Rockwell Hanford report RHO-LD-160 (1981), p. 45.

23. S. Shalev and J. M. Cuttler, *Nuclear Science and Engineering* 51, 52 (1973).

24. H. Franz, W. Rudolph, H. Ohm, K. L. Kratz, G. Herrmann, F. M. Nuh, D. R. Slaughter, and S. G. Prussin, "Delayed-Neutron Spectroscopy with ^{3}He Spectrometers," *Nuclear Instruments and Methods* 144, 253 (1977).